Bioorg. Med. Chem. 29 (2021) 115873

Contents lists available at ScienceDirect

Bioorganic & Medicinal Chemistry

journal homepage: www.elsevier.com/locate/bmc

Xanthones for melanogenesis inhibition: Molecular docking and QSAR studies to understand their anti-tyrosinase activity

G.P. Rosa [a,b], A. Palmeira [c,d], D.I.S.P. Resende [c,d], I.F. Almeida [e], A. Kane-Pagès [b], M. C. Barreto [a,b,*], E. Sousa [c,d,*], M.M.M. Pinto [c,d]

[a] cE3c–Centre for Ecology, Evolution and Environmental Changes/Azorean Biodiversity Group, 9501-801 Ponta Delgada, Portugal
[b] Faculdade de Ciências e Tecnologia, Universidade dos Açores, 9501-801 Ponta Delgada, Portugal
[c] Laboratório de Química Orgânica e Farmacêutica, Departamento de Ciências Químicas, Faculdade de Farmácia, Universidade do Porto, Portugal
[d] CIIMAR – Centro Interdisciplinar de Investigação Marinha e Ambiental, Avenida General Norton de Matos, S/N, 4450-208 Matosinhos, Portugal
[e] UCIBIO/REQUIMTE, MedTec-Laboratório de Tecnologia Farmacêutica, Departamento de Ciências do Medicamento, Faculdade de Farmácia, Universidade do Porto, Portugal

ARTICLE INFO

Keywords:
Xanthones
Melanogenesis
Anti-tyrosinase
QSAR
Docking

ABSTRACT

The human skin is constantly exposed to external factors that affect its integrity, UV radiation being one of the main stress factors. The repeated exposure to this radiation leads to increased production of Reactive Oxygen Species (ROS) which activate a series of processes involved in photoaging. Excessive UV exposure also exacerbates melanin production leading to a variety of pigmentation disorders. Xanthones are reported to exhibit properties that prevent deleterious effects of UV exposure and high levels of ROS in the organism, so in this work a wide library of xanthones with different patterns of substitution was synthesized and tested for their inhibitory activity against the skin enzymes tyrosinase, elastase, collagenase and hyaluronidase, many of which were evaluated for the first time. Most of the compounds were tyrosinase inhibitors, with the best one (xanthone **27**) presenting an IC_{50} of 1.9 μM, which is approximately 6 times lower than the IC_{50} of the positive control kojic acid. Concerning the other enzymes, only one compound presented IC_{50} lower than 150 μM in elastase inhibition (xanthone **14** = 91.8 μM) and none in collagenase and hyaluronidase inhibition.

A QSAR model for tyrosinase inhibitory activity was built using six molecular descriptors, with a partial negative surface area descriptor and the relative number of oxygen atoms being positively contributing to the tyrosinase inhibitory activity. Docking using AutoDock Vina shows that all the tested compounds have more affinity to mushroom tyrosinase than kojic acid. Docking results implied that the tyrosinase inhibitory mechanisms of xanthonic derivatives are attributed to an allosteric interaction. Taken together, these data suggest that xanthones might be useful scaffolds for the development of new and promising candidates for the treatment of pigmentation-related disorders and for skin whitening cosmetic products.

1. Introduction

As the protective barrier of the human body, the skin is constantly exposed to external factors like air pollutants and UV radiation. Repeated exposure to UV radiation leads to the formation of ROS, which initiate a series of processes involved in photoaging or extrinsic aging.[1] One of the skin's mechanisms of protection against UV radiation is the production of melanin. UV exposure triggers melanin synthesis within melanocytes on the basal layer of the skin activating the production of tyrosinase, the key enzyme of the melanin synthesis pathway. Melanin is then transported to keratinocytes and accumulates within keratinocytes and melanocytes in the perinuclear area as supranuclear "caps" that are thought to shield DNA from UV rays.[2] However, excessive UV exposure can lead to an exacerbated activation of tyrosinase production whose consequence is an excessive and non-uniform accumulation of melanin, leading to solar lentigo (liver-spots), melasma, or post-inflammatory hyperpigmentation (melanoderma). Due to its crucial role in melanin synthesis, tyrosinase inhibition is the main target of new agents for reduction of melanogenesis.[3]

The action of ROS formed by UV-exposure induces the expression of

* Corresponding authors at: cE3c–Centre for Ecology, Evolution and Environmental Changes/Azorean Biodiversity Group, 9501-801 Ponta Delgada, Portugal (M.C. Barreto). Laboratório de Química Orgânica e Farmacêutica, Departamento de Ciências Químicas, Faculdade de Farmácia, Universidade do Porto, Portugal (E. Sousa).
E-mail addresses: maria.cr.barreto@uac.pt (M.C. Barreto), esousa@ff.up.pt (E. Sousa).

https://doi.org/10.1016/j.bmc.2020.115873
Received 3 September 2020; Received in revised form 5 November 2020; Accepted 9 November 2020
Available online 19 November 2020

extracellular matrix degradation (ECM)-degrading enzymes, like collagenase (a matrix-metalloprotease (MMP)) or elastase,[4] by the activation of cytokine receptors on the cell surface of keratinocytes and dermal fibroblasts. The referred phenomenon leads to the breakdown of various components of the ECM, causing accumulation of fragmented collagen and elastin fibrils, which activate an inflammatory response.[5,6] The accumulation of these residues inhibits the synthesis of new collagen and elastin molecules, hindering the renewal of the ECM structure, which leads to the flaccidity of the skin and the appearance of wrinkles.[4] Other enzyme related with photo-induced skin aging is hyaluronidase. This enzyme breaks down hyaluronic acid, a glycosaminoglycan that binds water molecules retaining them in the tissues. In fact, 50% of all the hyaluronic acid present in the organism is located on the skin, being the main responsible for maintaining its moisture. When the action of ROS leads to over-expression of hyaluronidase, the increase in the breakdown of hyaluronic acid results in a drier and wrinkled skin.[7] As these consequences are related to a ROS-induced increase in the expression levels of tyrosinase, elastase, collagenase and hyaluronidase, these enzymes are considered preferred targets for developing anti-aging agents.[8]

Natural xanthones, displaying a common 9*H*-xanthen-9-one scaffold (Fig. 1), are considered ubiquitous polyphenolic compounds. Both natural and synthetic derivatives have been reported for skin applications.[9,10] Simple oxygenated xanthones have been reported to have antioxidant activity depending on the degree of oxygenation as well as the position of the substituents. This type of xanthones has shown scavenging activity against ROS as well as metal chelating capacity and inhibition of lipid peroxidation[11–13]. Regarding anti-aging activity, there are some reports of natural and complex xanthones very active against tyrosinase, like 3-aryl substituted xanthones[14] or pyranocycloartobiloxanthone A, a naturally-occurring xanthone,[15] or with anti-wrinkle activity, like α-mangostin.[16]

In a recent work, our group reported the anti-aging potential of a very limited group of polyoxygenated xanthones, some of them with interesting anti-tyrosinase activities.[17] Inhibition activities of enzymes related to skin photoaging (tyrosinase, collagenase, elastase, and hyaluronidase), were for the first time investigated for three simple hydroxylated xanthones, found to be extremely good tyrosinase inhibitors, with IC_{50} in the same order of magnitude and lower than the one obtained for the positive control kojic acid. Taking this information in account, the aim of the present work was to investigate a wider library of xanthones with diverse patterns of substitution, obtained by synthesis, for their anti-aging activities, namely the effects in the inhibition of tyrosinase, collagenase, elastase, and hyaluronidase. In addition, a quantitative structure-activity relationship (QSAR) model was built to establish a relationship between the structure of the referred xanthones and their tyrosinase inhibitory activity, which will allow a more straightforward design of new active compounds.

2. Results and discussion

2.1. Chemistry

Three traditional methods can be applied for the synthesis of simple xanthones (Table 1): the synthesis via condensation of a salicylic acid or salicylic ester with a phenol derivative (a), the synthesis via benzophenone (b), and the synthesis via diphenyl ether intermediates (c) (Scheme 1)[18,19]. Compounds **2**,[20] **6**[20] (Grover, Shah and Shah) and **33** (Eaton's reagent) were synthesized by via (a), while the compounds **3**,[20] **4**,[20] **7**,[20] **8**,[20] **12**,[20] **17-19**,[20] **26**[21] and **29**[21,22] were obtained by via (b). Compound **14**[23] was obtained through a dehydrative process (d) from commercial 2,2′,4,4′-tetrahydroxybenzophenone. The diaryl process has led to the synthesis of the compounds **10**[20] and **15**[20] by via (e) and the compounds **5**,[20] **9**,[20] **11**[20] and **16**[20] by via (f), respectively.

Further structural modifications were performed in compounds **14**, **26** and **29**, in order to extend the structural diversity of this library of compounds (Scheme 2) as previously reported[21,22]. 3,6-Dichloro-9*H*-xanthen-9-one (**32**) was obtained from **14**, by reaction with thionyl chloride.[24]

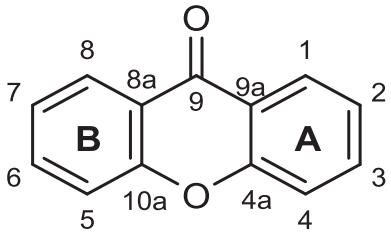

Fig. 1. Nucleus of xanthone.

2.2. In vitro enzyme inhibition analysis

The inhibition of tyrosinase, elastase, collagenase, and hyaluronidase activity by compounds **1**–**33** was evaluated in vitro and the results obtained are summarized in Table 2. A concentration of 150 μM was chosen as the maximum tested concentration and, in a first screening, all the compounds were tested at that concentration on the enzymatic assays. After the first screening, all the compounds which inhibited 50% or more of enzyme activity were assayed in a range of concentrations (serial dilutions) to obtain a dose/effect curve to determine the IC_{50} of each compound.

None of the 33 compounds assayed inhibited hyaluronidase activity, with the majority presenting inhibition levels of 3–5% (results not shown). In fact, in the literature there are no reports of xanthones with activity against this enzyme and a previous work from our group had already shown that three xanthone derivatives (**10**, **24**, and **25**) were inactive against hyaluronidase.[17]

Tyrosinase inhibition was the assay with most of the compounds tested being more active than the reference compound, kojic acid, which is a very good indication of their potential to become effective tyrosinase inhibitors. In fact, compounds **21**, **22**, and **31**–**33** presented an IC_{50} higher than the reference compound. The best results were obtained for compounds **26**, **27**, and **29**, with IC_{50} approximately 6 times lower than kojic acid, and in the same magnitude of derivative **25**, the hit compound[17] that led to the present structure–activity relationship (SAR) study. At a first glance, this might indicate that the presence of a methoxy substituent on C-3 and C-4, along with a methyl group on C-1 favours the inhibitory activity. The presence of two hydroxyl groups also seems to be associated with the increase of inhibitory activity, what can be inferred from the results obtained for compounds **10**–**14**. Also, the presence of a hydroxyl and a methoxy group in *ortho* positioning on ring A is associated with a higher inhibitory activity (compounds **18**–**20**). Compounds **31**–**33** were those with the lowest activity against tyrosinase. It is interesting to observe that between compounds **30** and **31** (Table 1), the only difference is the presence of a OCH_3 group on C-6; however, their activity is very different – while the IC_{50} of compound **30** is 3.37 μM, for compound **31** that value is higher than 150 μM. This indicates that the OCH_3 group on C-6 impairs in **31** the inhibitory capacity of the compound.

The obtained anti-tyrosinase activity of this library of xanthonic derivatives allowed a SAR analysis (Fig. 2). In general, OCH_3 and OH increase activity when in R^1, R^2, R^3, R^4, and/or R^6 (two or three OCH_3/OH groups are favourable), although, anti-tyrosinase activity was also noted for the unsubstituted xanthone **1**. Group CH_3 in R^1 together with OCH_3 in two or three positions (R^3, R^4, R^6), is more favourable than a triple substitution with OH, which in turn is more favourable than a double substitution with OH (R^3 and R^4). Similarly, CHO in R^1 is very favourable when together with a OCH_3 double substitution at R^3 and R^4; this increase in activity is not so pronounced when the double substitution in R^3 and R^4 is with an OH. When a $CHBr_2$ is at R^1, an increase in

Table 1
Structure of xanthones **1**–**33**.

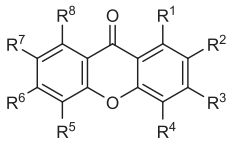

Comp.	R^1	R^2	R^3	R^4	R^5	R^6	R^7	R^8	Comp.	R^1	R^2	R^3	R^4	R^5	R^6	R^7	R^8
1	H	H	H	H	H	H	H	H	**18**	H	H	OH	OCH_3	H	H	H	H
2	OH	H	H	H	H	H	H	H	**19**	H	H	OCH_3	OH	H	H	H	H
3	H	OH	H	H	H	H	H	H	**20**	OH	OCH_3	OH	H	H	H	H	H
4	H	H	OH	H	H	H	H	H	**21**	CHO	H	OH	OH	H	H	H	H
5	H	H	H	OH	H	H	H	H	**22**	CHO	H	OCH_3	OCH_3	H	H	H	H
6	OCH_3	H	H	H	H	H	H	H	**23**	CHO	H	OCH_3	OCH_3	H	OCH_3	H	H
7	H	OCH_3	H	H	H	H	H	H	**24**	CH_3	H	OH	OH	H	H	H	H
8	H	H	OCH_3	H	H	H	H	H	**25**	CH_3	H	OH	OH	H	OH	H	H
9	H	H	H	OCH_3	H	H	H	H	**26**	CH_3	H	OCH_3	OCH_3	H	H	H	H
10	OH	OH	H	H	H	H	H	H	**27**	CH_3	Cl	OCH_3	OCH_3	H	H	H	H
11	H	OH	OH	H	H	H	H	H	**28**	CH_3	Br	OCH_3	OCH_3	H	H	H	H
12	H	H	OH	OH	H	H	H	H	**29**	CH_3	H	OCH_3	OCH_3	H	OCH_3	H	H
13	OH	H	H	H	H	H	OH	H	**30**	$CHBr_2$	H	OCH_3	OCH_3	H	H	H	H
14	H	H	OH	H	H	OH	H	H	**31**	$CHBr_2$	H	OCH_3	OCH_3	H	OCH_3	H	H
15	OCH_3	OCH_3	H	H	H	H	H	H	**32**	H	H	Cl	H	H	Cl	H	H
16	H	OCH_3	OCH_3	H	H	H	H	H	**33**	OH	H	CH_3	H	H	CH_3	H	OH
17	H	H	OCH_3	OCH_3	H	H	H	H									

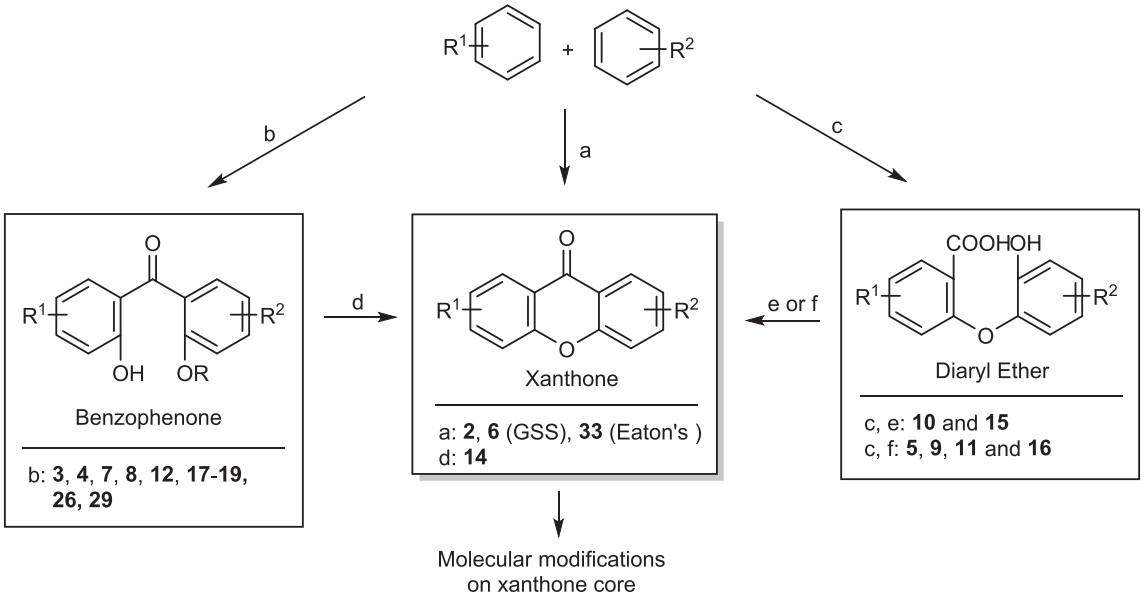

Scheme 1. Classical methods for the synthesis of xanthones used in this study. Adapted from[20].

activity is observed in combination with two OCH_3 (R^3, R^4), but with three OCH_3 (R^3, R^4, R^6) this activity decreases. In position R^2, the Br substituent causes a small decrease in activity, while the Cl is favourable in R^2, but it severely decreases activity when in R^3 and R^6. OH in both R^1 and R^8 decreases activity. In general, for mono and disubstituted xanthones, the nature and the position of the substituent (OCH_3, OH) did not affect significantly the anti-tyrosinase activity, except for the case of the dichloro derivative **32** which was inactive. Among trisubstituted xanthones, methoxy groups were generally more well-tolerated than hydroxy groups and for higher degrees of substitution, it was difficult to stablish conclusive SAR due to the heterogeneity of the substituents.

As referred above, other authors have described other xanthone derivatives with anti-tyrosinase activity, like 3-aryl substituted xanthones[14] or pyranocycloartobiloxanthone A[15]. The most active 3-aryl xanthone was 1-hydroxy-3-(4-hydroxyphenyl)-9*H*-xanthen-9-one with an IC_{50} of 11.3 ± 0.16 μM[14] which is less active than most of the compounds tested, and similarly to its parent compound, 1-hydroxyxanthone (**2**) (Table 2). This means that the introduction of an aryl group (with different substituents) on the C-3 position of the xanthone moiety, does not favour tyrosinase inhibition. It is not possible to compare the results with those obtained for pyranocycloartobiloxanthone A because only the % of inhibition at a much higher concentration than the one employed in this work was presented.[15]

None of the compounds tested inhibited more than 50% of collagenase activity at 150 μM, with almost half of the compounds tested presenting an inhibitory activity higher than 30%, at that concentration. The other half inhibited mostly 15–29% of collagenase activity (Table 2). Compound **8** was the most active against collagenase, inhibiting about 42% of collagenase activity. Compound **33** had the worst activity of the whole library, having inhibited less than 0.5% of collagenase activity at the maximum concentration tested. Since most of the results range between 15 and 35%, a SAR analysis was not feasible.

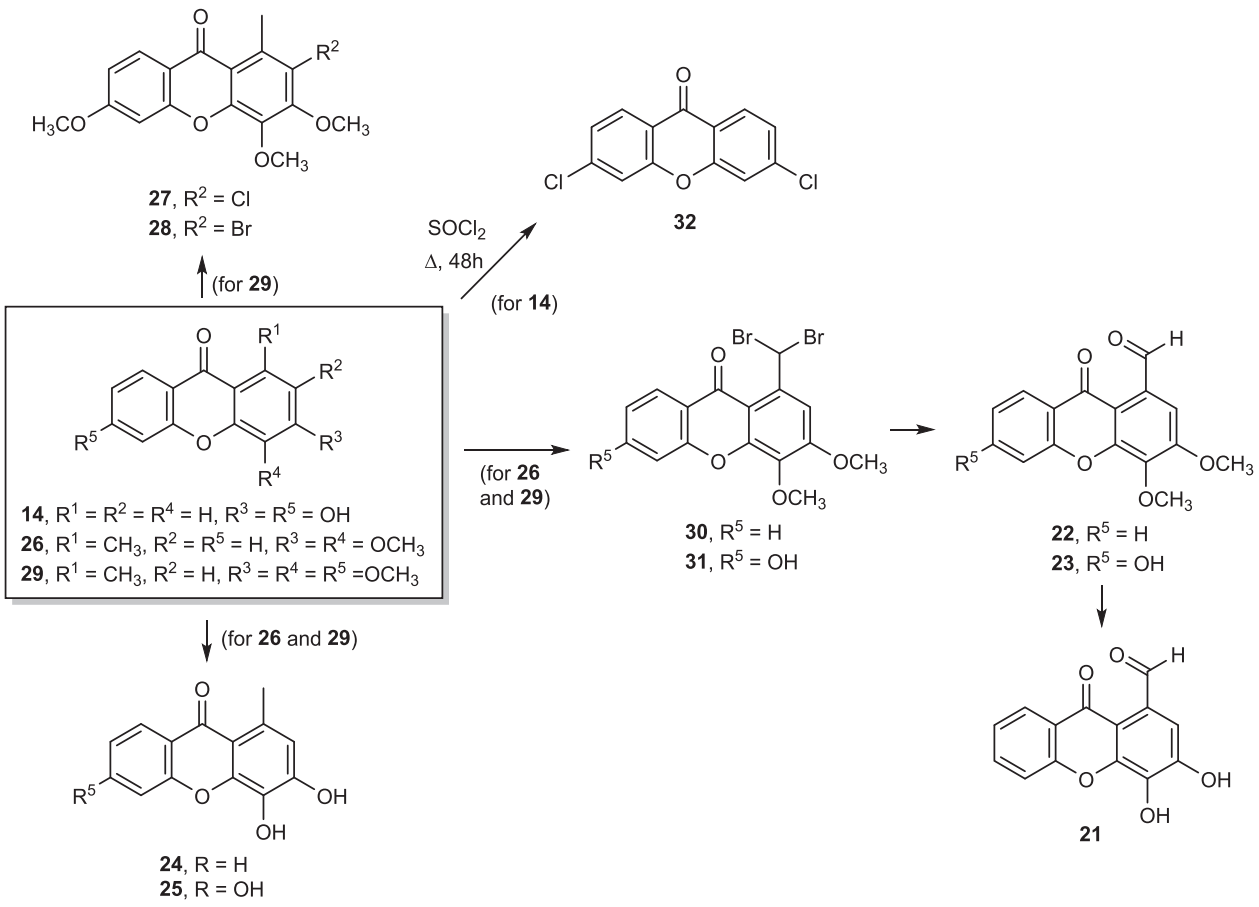

Scheme 2. Structural modifications on xanthones **14**, **26**, and **29**.

For elastase inhibition, the results were not very promising, with compound **14** being the only one with IC_{50} lower than the maximum concentration tested (Table 2). The IC_{50} obtained for compound **14** (91.8 ± 1.35 μM) is considerably high, especially considering the value obtained for the reference compound (0.26 ± 0.003 μM). At the maximum concentration tested, a good part of the library of compounds inhibited 20–45% of elastase activity, while the remaining presented low inhibition (0–20%). According to the results, the presence of hydroxyl groups on both aromatic rings (compound **14**) doubles the inhibitory capacity of xanthones when compared to xanthones with hydroxyl substituents on only one ring.

This is the first time that a library of xanthone derivatives is tested for their inhibitory activity of these enzymes, despite the low results obtained for elastase, collagenase, and hyaluronidase. However, it is undeniable that the xanthones studied have a great potential to be effective tyrosinase inhibitors. To better understand the mechanism of action and the effect of different substituents of these xanthone derivatives, molecular docking studies and QSAR analysis were developed.

2.3. QSAR model

With the overall biochemical results, a QSAR model was built to establish a relationship between the structure of the xanthone derivatives and their tyrosinase inhibitory activity, which will guide the rational design of new active compounds.[25] The correlation coefficient (R^2) (a statistical measure of how close the data are to the fitted regression line), standard error (s) (which consists of an absolute measure of the quality of fit), and Fisher's value (F) (which represents the F-ratio between the variance of actual and predicted activity), were employed to evaluate the validity of regression equation.[26] A relevant point in developing QSAR model is the number of descriptors used to elaborate the equation. Laws of QSAR establish that it should be one descriptor for each five molecules.[26] Therefore, as the training set was composed of 30 molecules, 6 descriptors were used to build the QSAR models. The final model was further validated using the test set. The multilinear regression analysis using Heuristic method for 30 compounds in the six-parameter model is given in Fig. 3.

The best training model had a coefficient of determination (R^2) of 0.9051, Fisher value of 36.57, and S of 5.94, which demonstrate that the proposed model has satisfactory statistical stability and validity in spite of the small group of molecules used to build the model. The squared correlation coefficient R^2 is a relative measure of quality of fit by regression equation. Correspondingly, it represents more than 90% of the total variance ($R^2 = 0.9051$) in anti-tyrosinase activity exhibited by xanthone derivatives. Its value is close to 1.0 which represents the better fit to the regression line.[27] The F-test reflects the ratio of the variance explained by the model and the variance due to the error in the regression. High value of the F-test indicates that the model is statistically significant. The QSAR model is significant at 95% level as shown by their Fischer ratio values which exceed the tabulated values (2.53) as desired for a meaningful correlation.[28] Standard deviation expresses the variation of the residuals or the variation about the regression line. Thus standard deviation is an absolute measure of quality of fit and should have a low value for the regression to be significant.[28] External (test set) predictivity was used as validation criteria, and the model was able to predict the anti-tyrosinase activity with an average difference of 18.3 from the experimental value.[29]

The WNSA-3 Weighted PNSA, the relative number of oxygen atoms and PPSA-3 Atomic charge weighted PPSA are positively correlated with the predicted tyrosinase inhibitory activity. By analysing the QSAR model, the most representative descriptor is WNSA-3 Weighted PNSA with a positive coefficient and the highest *t*-test value. WNSA-3

Table 2
Tyrosinase, elastase, and collagenase inhibition activity of xanthones **1**–**33**.

	Anti-Tirosinase		Anti-Elastase		Anti-Collagenase	
Comp.	% Inhibition 150 μM	IC_{50} (μM)	% Inhibition 150 μM	IC_{50} (μM)	% Inhibition 150 μM	IC_{50} (μM)
1	84.90 ± 2.60	8.84 ± 0.270 ^{a,b}	12.31 ± 0.64^{a}	–	37.03 ± 2.76^{a,b,c}	–
2	85.00 ± 1.40	8.83 ± 0.150 ^{a,b,c}	23.87 ± 1.02^{b,c}	–	34.45 ± 2.77^{a,b,c,d}	–
3	89.32 ± 0.37	5.60 ± 0.020 ^{e,f}	24.18 ± 0.99^{b,c}	–	36.68 ± 1.48^{a,b,c,d}	–
4	81.01 ± 1.20	9.26 ± 0.140 ^{a}	21.57 ± 0.54^{b}	–	37.08 ± 2.03^{a,b,c}	–
5	88.64 ± 2.23	8.46 ± 0.210^{b,c}	25.03 ± 0.65^{c,d}	–	33.83 ± 1.19^{a,b,d}	–
6	97.29 ± 0.89	5.14 ± 0.050^{f}	17.14 ± 0.08^{e}	–	32.68 ± 1.83^{a,d,f,g}	–
7	88.60 ± 0.80	8.47 ± 0.080^{b,c}	15.87 ± 0.09^{e}	–	35.41 ± 2.15^{a,b,c,d}	–
8	97.40 ± 2.12	5.14 ± 0.110^{f}	19.95 ± 0.97^{f}	–	42.05 ± 2.21^{p}	–
9	93.80 ± 1.88	5.33 ± 0.110^{e,f}	18.47 ± 0.54^{e,f}	–	31.91 ± 0.70^{d,f,g}	–
10*	*96.17 ± 0.88*	*7.8 ± 0.070*^{d}	*35.2 ± 1.84*^{g,h,i}	–	*35.77 ± 1.82*^{a,b,c,d}	–
11	96.15 ± 0.15	5.7 ± 0.670^{e}	36.87 ± 0.65^{h,I,j}	–	38.80 ± 1.09^{c,p}	–
12	97.61 ± 1.29	5.12 ± 0.070^{f}	43.96 ± 0.97^{k}	–	35.43 ± 2.01^{a,b,c,d}	–
13	99.59 ± 0.22	4.52 ± 0.010^{g}	39.1 ± 0.98^{j,l}	–	38.07 ± 0.63^{b,c,p}	–
14	99.54 ± 0.21	4.42 ± 0.010^{g}	83.35 ± 1.06^{m}	91.8 ± 1.35	35.29 ± 1.28^{a,b,c,d}	–
15	99.42 ± 0.26	4.02 ± 0.010^{g,h}	29.62 ± 0.21^{n}	–	33.81 ± 2.40^{a,b,d}	–
16	90.50 ± 2.57	8.29 ± 0.230^{c,d}	28.89 ± 0.69^{n}	–	33.13 ± 1.69^{a,d,f}	–
17	97.62 ± 0.88	5.12 ± 0.050^{f}	29.87 ± 0.98^{n}	–	23.03 ± 1.46^{h,i,j}	–
18	99.63 ± 0.22	3.81 ± 0.010^{h,i}	33.02 ± 0.67^{g}	–	34.41 ± 0.93^{a,b,c,d}	–
19	96.18 ± 2.99	5.2 ± 0.160^{e,f}	34.12 ± 0.85^{g,h}	–	26.42 ± 0.60^{h,i,k}	–
20	99.82 ± 0.20	3.01 ± 0.010^{j}	40.1 ± 1.9^{l}	–	24.66 ± 0.77^{h,i,j,k}	–
21	83.92 ± 0.42	89.37 ± 0.440^{l}	5.98 ± 0.01^{o}	–	25.30 ± 1.86^{h,i,k}	–
22	99.57 ± 0.36	29.13 ± 0.110^{m}	2.11 ± 0.01^{p}	–	28.85 ± 0.18^{f,g,k}	–
23	91.77 ± 0.59	3.16 ± 0.020^{j}	1.97 ± 0.03^{p}	–	28.18 ± 1.83^{g,k}	–
24*	*84.05 ± 1.87*	*8.93 ± 0.160*^{a,b}	*10.85 ± 0.39*^{a}	–	*26.83 ± 1.45*^{h,k}	–
25*	*91.42 ± 0.23*	*3.28 ± 0.010*^{i,j}	*18.21 ± 0.71*^{e,f}	–	*24.91 ± 0.93*^{h,i,j,k}	–
26	99.93 ± 0.10	2 ± 0.001^{k}	17.08 ± 0.91^{e,h}	–	20.11 ± 0.39^{j,l}	–
27	99.80 ± 0.18	1.9 ± 0.003^{k}	36.21 ± 1.08^{i}	–	23.96 ± 1.96^{h,i,j,k}	–
28	89.77 ± 0.51	5.57 ± 0.030^{e,f}	27.54 ± 1.3^{d}	–	21.62 ± 0.38^{i,j}	–
29	98.39 ± 0.30	2.24 ± 0.007^{k}	12.54 ± 0.25^{a}	–	7.80 ± 0.90^{m}	–
30	98.96 ± 0.35	3.37 ± 0.010^{i,j}	37.15 ± 0.98^{i,j}	–	15.61 ± 0.96^{l,n}	–
31	35.97 ± 0.54	–	36.52 ± 0.96^{h,I,j}	–	13.45 ± 0.77^{n}	–
32	40.12 ± 0.12	–	16.54 ± 0.84^{e}	–	9.72 ± 0.20^{m}	–
33	47.32 ± 0.22	–	24.12 ± 0.54^{b,c}	–	0.38 ± 0.09^{o}	–
Kojic acid	–	12.81 ± 0.01^{n}	–	–	–	–
MAAPVCK	–	–	–	0.26 ± 0.003	–	–
EDTA	–	–	–	–	–	102.95 ± 5.30

Kojic acid (for tyrosinase), MAAPVCK (for elastase), and EDTA (for collagenase) were used as positive controls. In each column, different letters indicate significant differences in the activity of compounds ($p < 0.05$). * Compounds data previously reported in[17].

Weighted PNSA is a charged partial surface area descriptor, characterizing the partial negative surface area. In this model, the relative number of oxygen atoms and PPSA-3 Atomic charge weighted PPSA, which represents the atomic contribution of atoms with positive partial charge to the molecular surface area, also positively contribute to the tyrosinase inhibitory activity.[30,31] The Kier and Hall index, ZX Shadow/ZX Rectangle, and HA dependent HDSA-1/TMSA have negative coefficients, being negatively correlated with the tyrosine inhibitory activity. The Kier and Hall index is a molecular connectivity index that emphasizes different aspects of atom connectivity within a molecule, the amount of branching ring structures present and flexibility.[32] ZX Shadow/ZX Rectangle characterizes the molecular shape within a ZX plane; and HA dependent HDSA-1/TMSA is the area weighted surface charge of hydrogen bonding donor atoms.[30] From all the above, it can be concluded that the QSAR model is applicable for tyrosinase inhibitory activity, which suggests that the model may have predictive capacity for more hits.

As non-competitive and mixed-inhibition are frequent modes observed in kinetics studies on tyrosinase activities, a kinetic study was performed. Among the hit compounds, an hydroxylated (**25**) and a metoxylated (**26**) xanthonic derivative were chosen to conduct this study, due to their high synthetic accessibility. The kinetic analysis (Table 3) of tyrosinase activity by compounds **25** and **26** points out to an uncompetitive inhibition, with V_{max} and K_M values decreasing when inhibitor concentration increases (Table 3), while the inhibition by kojic acid is confirmed as being mixed, implying that inhibition by these compounds is not limited to the active site.

To better understand the results obtained in the kinetic study, an *in silico* docking study was performed using the already available 3D structure of the mushroom *A. bisporus* tyrosinase[33] that would allow a more thorough study of the interactions between the active and allosteric sites and its substrates or inhibitors (Table 4). Tyrosinase, also known as monophenol monooxygenase, is a copper enzyme that is widespread among microorganisms, plants and animals. It catalyses the *o*-hydroxylation of phenols to catechols and the oxidation of catechols to quinones.[34] Mushroom tyrosinase contains two nonidentical cupric ions that are each coordinated by three imidazole rings from three histidine residues.[35] The mushroom tyrosinase is a heterotetrameric protein formed by two L subunits whose junction is still not clear, and two H subunits containing the two dicupric clusters that are responsible for catalytic activity.[33] Besides, tyrosinase also has two allosteric sites, and it has been describe that the known tyrosinase inhibitor kojic acid is a catalytic and allosteric tyrosinase inhibitor,[36] and kinetic results have pointed out to a mixed inhibition by this compound,[37] which is in accordance with the results obtained herein. Moreover, phtalic and cinnamic acids are also mixed-type inhibitors as also confirmed by kinetic studies, as when the catalytic site is occupied by a substrate or inhibitor, they bind to alternative locations (allosteric binding sites 1 and 2)[38,39] (Figure 4A). Thus, kojic acid, cinnamic acid, and phthalic acid were used to validate the docking study of the xanthonic derivatives, a class of compounds already described for their potential tyrosinase inhibitory and antioxidant activities.[15,40] The binding

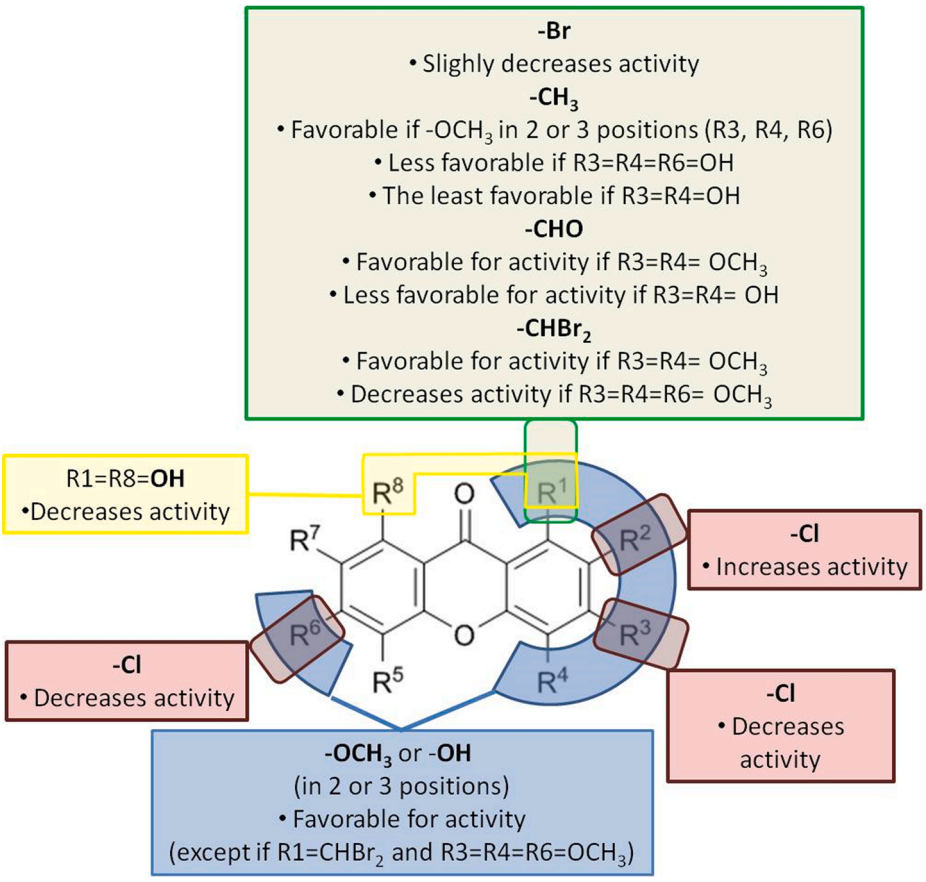

Fig. 2. Structure-activity relationship (SAR) analysis of xanthone derivatives with anti-tyrosinase activity.

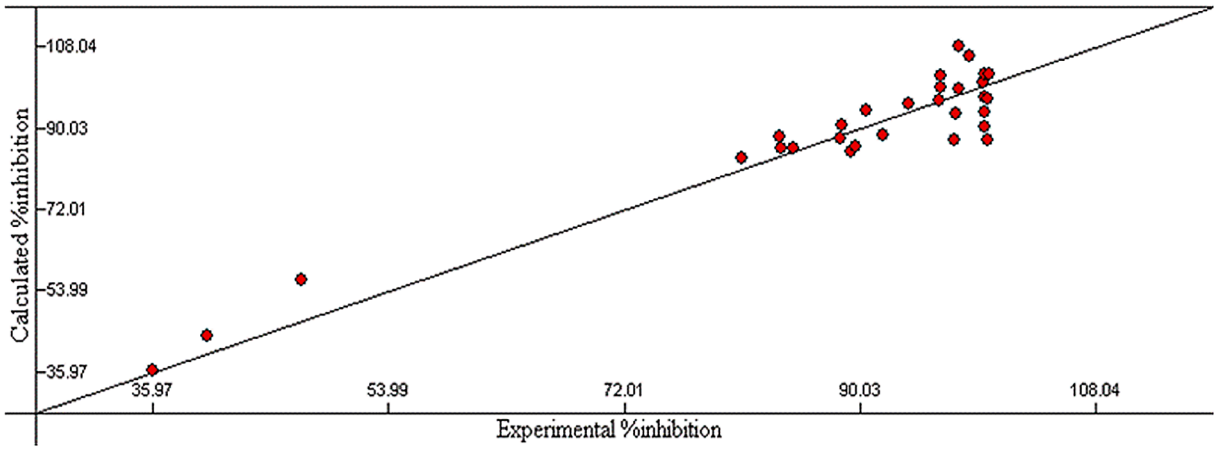

Nr	X	ΔX	t-test	Name of the descriptor
0	198.42	31.58	6.28	Intercept
1	5.15	0.91	5.63	WNSA-3 Weighted PNSA (PNSA3*TMSA/1000)
2	322.77	123.74	2.60	Relative number of O atoms
3	-12.91	2.29	-5.63	Kier&Hall index (order 2)
4	-115.22	34.42	-3.34	ZX Shadow / ZX Rectangle
5	-143.35	45.94	-3.12	HA dependent HDSA-1/TMSA
6	3.60	1.52	2.36	PPSA-3 Atomic charge weighted PPSA

Fig. 3. QSAR model obtained with the heuristic method for 30 xanthones with the CODESSA software ($R^2 = 0.9051$, $F = 36.57$, and $s = 5.94$). X, ΔX and *t*-test are the regression coefficient of the linear model, standard errors of the regression coefficient, and the t significance coefficient of the determination, respectively.

Table 3
Kinetic parameters of tyrosinase in the presence of increasing concentrations of inhibitors.

Compound	[Inhibitor] μM	V_{max} (Δ Abs/min)	K_m (mM)	Inhibition Type
25	0	0.0042 ± 0.0002[a]	0.070 ± 0.004[a]	Uncompetitive
	1.65	0.0037 ± 0.0002[a,b]	0.063 ± 0.004[a,b]	
	3.30	0.0035 ± 0.0004[b]	0.051 ± 0.011[b]	
	6.60	0.0032 ± 0.0002[b,c]	0.046 ± 0.009[b,c]	
	13.2	0.0028 ± 0.0001[c]	0.028 ± 0.003[c]	
26	0	0.0042 ± 0.0002[a,]	0.070 ± 0.004[a]	Uncompetitive
	2.0	0.0036 ± 0.0003[b]	0.053 ± 0.001[b]	
	4.0	0.0031 ± 0.0002[b]	0.041 ± 0.001[b]	
	8.0	0.0025 ± 0.0001[c]	0.027 ± 0.009[d]	
	16.0	0.0019 ± 0.0002[d]	0.026 ± 0.001[d]	
Kojic Acid	0	0.0042 ± 0.0002[a]	0.070 ± 0.004[a]	Mixed
	3.20	0.0038 ± 0.0001[a]	0.069 ± 0.002[a]	
	6.40	0.0030 ± 0.0002[b]	0.077 ± 0.001[b]	
	12.8	0.0025 ± 0.0002[c]	0.083 ± 0.002[c]	
	25.6	0.0019 ± 0.0001[d]	0.087 ± 0.001[d]	

In each section of each column, different letters indicate significant differences in the kinetic parameters ($p < 0.05$).

between the active site of mushroom tyrosinase and the test and control molecules was simulated using AutoDock Vina.

Docking results show that 26 out of the 33 tested compounds combine with mushroom tyrosinase preferably at the allosteric binding site 2, as stated by the higher binding affinities (i.e., lower docking scores) when compared to the catalytic site and the allosteric site 1. Moreover, 31 out of the 33 test xanthones presented higher binding affinities towards the allosteric site 2 than known allosteric site 2 binder cinnamic acid (−6.3 kCal.mol^{-1}).[38] Kojic acid, a mixed-type inhibitor,[37] binds more strongly to the catalytic site (−5.5 kCal.mol^{-1}), followed by the allosteric site 2 (-5.2 kCal.mol^{-1}). Based on enzyme kinetic studies, **25** and **26** exerted a noncompetitive-type inhibition; the higher binding affinity of **25** (−8.0 kCal.mol^{-1}) and **26** (−7.2 kCal.mol^{-1}) to the allosteric site 2 is in accordance to this allosteric inhibitory profile. Figure 4 shows top score docked conformation of test compounds, with detailed analysis of compounds **25** and **26** in the allosteric site 2 of tyrosinase.

Cinnamic acid established four polar interactions with residues Asn-310, Asp-312, Val-313, and Gln-307, which is in agreement with previously reported docking and molecular dynamics studies[38,39]; it also establishes *T*-shaped π-stacking interactions with Trp-358 (Figure 4B). Compound **25** established four polar interactions (Gln-307, Lys-379, Asp-357 and Glu-359); parallel π-stacking interactions also occurred between the xanthonic tricyclic ring system and Trp-358 (Figure 4C). Compound **26** forms 3 polar interactions (Gln-307, Lys-379, Asp-357), a parallel-displaced π-stacking interaction (Trp-358) and a C—H···π interaction[41] (Phe-368) (Figure 4D). In conclusion, three anchoring points seem relevant for xanthonic derivatives polar interactions (Gln-307, Lys-379, and Asp-357), with additional π-stacking interactions (Trp-358) further strengthening the affinity towards the allosteric pocket.

As in agreement with the QSAR model, not only the partial negative surface area and relative number of oxygen atoms contribute to activity,

Table 4
Docking scores of 33 xanthonic derivatives and known tyrosinase inhibitors on tyrosinase binding site (pdb code 2y9x).

	Docking Scores (kCal.mol^{-1})		
	Catalytic site	Allosteric site 1	Allosteric site 2
1	−6.8	−5.8	−7.1
2	−7.4	−5.4	−7.2
3	−6.8	−5.5	−7.3
4	−7.1	−6	−7.2
5	−7.5	−5.8	−7.3
6	−7.3	−5.5	−7.1
7	−6.8	−5.6	−8
8	−6.9	−5.7	−7.6
9	−7	−4.9	−7.4
10	−7	−6.2	−7.8
11	−7.1	−4.7	−7.8
12	−7.6	−5.6	−7.7
13	−7.3	−5.9	−7.6
14	−7.3	−5.8	−7.7
15	−6.5	−5.2	−7.2
16	−6.8	−5.1	−8
17	−6.7	−4.1	−7.6
18	−6.8	−4.4	−7.5
19	−7.2	−5.6	−7.7
20	−6.8	−5	−8.1
21	−7.9	−4.9	−7.3
22	−5.9	−4	−7.2
23	−6.5	−4.2	−7.3
24	−7.4	−5.6	−7.4
25	−7.9	−5.9	−8.0
26	−6.2	−3.3	−7.2
27	−6.3	−3	−7.0
28	−6.3	−3.1	−6.7
29	−6.8	−3.2	−7.2
30	−6.1	−2.3	−6.2
31	−6.2	0.8	−6.1
32	−6.7	−4.6	−6.8
33	−6.9	−5.6	−6.9
Kojic acid	−5.5	−4.5	−5.2
Cinnamic Acid	−5.8	−4.7	−6.3
Phtalic acid	−6.4	−5.9	−5.1

but also the substitution pattern seems to be influencing activity. Docking results implied that the tyrosinase inhibitory mechanisms of xanthonic derivatives is attributed to an allosteric mechanism of action. It is hypothesized that, in the presence of a tyrosinases substrate, such as tyrosine, the xanthonic derivatives occupy non-catalytic binding sites.

3. Conclusions

The results obtained in this study show that tested xanthone derivatives can behave as tyrosinase inhibitors, with most of the compounds studied being more potent than the commercially used kojic acid, showing the ability for application on cosmetic formulations and treatment of pigmentation disorders. Regarding the inhibition of other enzymes related with photoaging, the xanthone derivatives tested were not very effective. However, it must be valued that this is the first time such a kind of library of xanthonic derivatives was tested for activity against elastase, collagenase, and hyaluronidase. According to the QSAR model and docking studies, it can be concluded that the partial negative surface area, the relative number of oxygen atoms and the substitution pattern of the xanthonic core, allowing interaction with residues on the allosteric binding site, contribute to the tyrosinase inhibitory activity. These structural characteristics will allow a more rational design of new xanthonic derivatives with application, in a near future, as skin anti-aging agents.

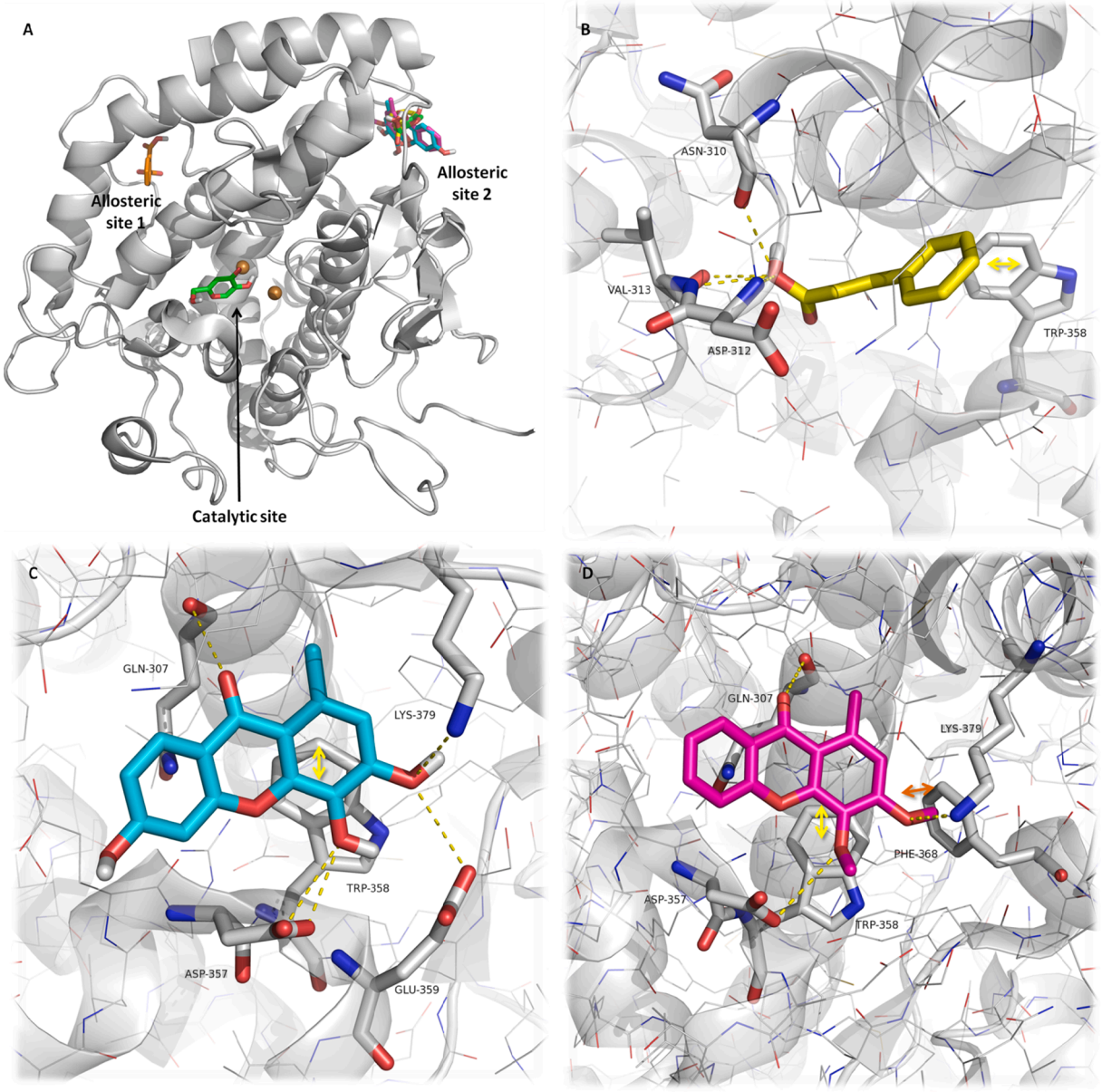

Fig. 4. Docking prediction of binding poses of known tyrosinase inhibitors kojic, phtalic and cinnamic acid, and test compounds **25** and **26**. (A) Top score docking poses of kojic acid (green sticks) on catalytic site, phthalic acid (orange sticks) on allosteric site 1, and cinnamic acid on allosteric site 2 (yellow sticks) are shown as exemplification to better locate the different binding pockets on the tyrosinase 3D structure; compounds 25 (light blue sticks) and 26 (magenta sticks) top poses are represented on allosteric site 2. Tyrosinase (pdb code 2y9x) is represented as ribbon. The spheres represent the copper ions. Close view of docking pose of the know allosteric inhibitor cinnamic acid (B), compounds 25 (C), and compound 26 (D), in the tyrosinase allosteric pocket 2. Ligand and core amino acid residues are displayed as sticks. Hydrogen interactions are represented with yellow broken lines. π Interactions and C—H π interactions are represented with yellow double arrow and orange double arrow, respectively.

4. Experimental part

4.1. Materials and methods

Xanthone (**1**) was purchased from Sigma-Aldrich, and the oxygenated xanthones **2**-**12**,[20] **13**,[23] **14**,[23] **15**-**21**,[20] **22**,[21] **23**,[42] **24**,[22] **25**,[22] **26**,[21] **27**,[42] **28**,[22] **29**,[42] **30**,[21] **31**,[42] and **33**[17] were synthesized as described before.

Tyrosinase, L-tyrosine, kojic acid, monosodium phosphate, sodium phosphate dibasic elastase, *N*-methoxysuccinyl-Ala-Ala-Pro-Val-*p*-nitroanilide, *N*-methoxysuccinyl-Ala-Ala-Pro-chloro, 2-[4-(2-hydroxyethyl)piperazin-1-yl]ethanesulfonic acid (HEPES), *N*-[3-(2-furyl) acryloyl]-Leu-Gly-Pro-Ala (FALGPA), *N*-[tris(hydroxymethyl)methyl]-2-aminoethanesulfonic acid (TES) sodium salt, ninhydrin, citric acid, sodium citrate, EDTA, hyaluronidase, hyaluronic acid, calcium chloride, sodium aurothiomalate, potassium metaborate, 4-dimethylaminobenzaldehyde (DMAB), sodium acetate, acetic acid, and hydrochloric acid were purchased from Sigma-Aldrich. Collagenase was supplied by Merck. Tin (II) chloride was obtained from Riedel-deHaën. The water used in all experiments was purified water obtained using a Direct-Q Water Purification System (Merck Millipore) with a reverse osmosis process.

4.2. Synthesis of 3,6-dichloro-9H-xanthen-9-one (32)

3,6-Dihydroxy-9*H*-xanthen-9-one (**14**, 0.200 g, 876 μmol) was dissolved in thionyl chloride (15 ml, 0.21 mol) and the reaction mixture was refluxed for 48 h. After cooling to room temperature, the reaction

was carefully quenched with water. The organic phase was extracted with CH_2Cl_2, washed with saturated Na_2CO_3 (aq.) and water to give the crude product which was then purified by column chromatography using a mixture of EtOAc/Hexane (3:7) as mobile phase.

3,6-Dichloro-9*H*-xanthen-9-one (**32**); White solid (0.188 g, 81% yield); m.p.: 165–168 °C; ^{1}H NMR (Lit.[43]) (300 MHz, $CDCl_3$, δ ppm): 8.25 (2H, d, $^3J_{1,2} = {}^3J_{8,7} = 8.6$ Hz, H-1, H-8), 7.50 (2H, d, $^4J_{4,2} = {}^4J_{5,7} = 1.9$ Hz, H-4, H-5), 7.36 (2H, dd, $^3J_{2,1} = {}^3J_{7,8} = 8.6$ Hz and $^4J_{2,4} = {}^4J_{7,5} = 1.9$ Hz, H-2, H-7) ppm.

4.3. Enzyme inhibition assay

4.3.1. Tyrosinase inhibition assay

This activity was assayed by an adaptation of the tyrosinase inhibition method described by Shimizu et al.[44] and modified by Manosroi et al.[45] Briefly, 25 μL of tyrosinase enzyme solution (135 U/mL), 25 μL of ten serial concentrations of the compounds (0.3–150 μM dissolved in 0.1 M phosphate buffer pH 6.8 containing no more than 2.5% DMSO) and 100 μL phosphate buffer were mixed in a 96-well plate and incubated at 37 ± 2 °C for 20 min. Then, 50 μL of 1.66 mM of tyrosine solution in 0.1 M phosphate buffer (pH 6.8) were added. The enzyme activity was measured at 490 nm every 10 min for 30 min in a Bio Rad Model 680 Microplate Reader (Bio-Rad Laboratories, Inc., Hercules, CA, USA). Kojic acid was used as positive control. The experiments were done in triplicate. For each concentration, enzyme activity was calculated as a percentage of the velocities compared to that of the assay using buffer without any inhibitor. The IC_{50} value was determined as the concentration of compound that inhibited 50% of enzyme activity. The mode of inhibition and inhibition parameters of the compounds, i.e. the Michaelis–Menten constant (Km), maximal velocity (Vmax), were determined by Lineweaver–Burk plot analysis using various concentrations of L-tyrosine.

4.3.2. Elastase inhibition assay

The compounds were assayed by the method described by Ndlovu et al.[46] with some modifications. Briefly, 25 μL of elastase enzyme solution (0.3 U/mL), 50 μL of ten serial concentrations of the compounds (0.3–150 μM dissolved in 0.1 M HEPES buffer pH 7.5 containing no more than 2.5% DMSO) and 125 μL HEPES buffer were mixed in a 96-well plate and incubated at room temperature for 20 min. Then, 50 μL of *N*-methoxysuccinyl-Ala-Ala-Pro-Val-*p*-nitroanilide (1 mM) were added. The enzyme activity was measured at 405 nm in the moment of substrate addition and after 40 min of incubation at 25 °C in a Bio Rad Model 680 Microplate Reader (Bio-Rad Laboratories, Inc., Hercules, CA, USA). *N*-Methoxysuccinyl-Ala-Ala-Pro-chloro was used as positive control. The experiments were done in triplicate. For each concentration, enzyme activity was calculated as a percentage of the velocities compared to that of the assay using buffer without any inhibitor. The IC_{50} value which was the concentration of the sample that inhibited 50% of the enzyme activity was determined.

4.3.3. Collagenase inhibition assay

An adaptation of the method of Moore and Stein[47] with modifications by Mandl et al.[48] was used to determine anticollagenase activity. To 2 ml test tubes was added: 25 μL of collagenase solution (0.8 U/mL), 25 μL TES buffer (50 mM) with 0.36 mM calcium chloride (pH 7.4) and 50 μL of test sample or the reference compound EDTA (with concentrations ranging between 9.4 and 150 μM). The tubes were incubated in a water bath at 37 °C for 20 min. Thereafter, 50 μL FALGPA (1 mM) solution was added to the tubes and incubated further for 60 min at 37 °C. To all tubes, 200 μL of a solution containing equal volumes of a 1.6 mg/mLTin chloride (II) solution in 200 mM citrate buffer (pH 5) and 50 mg/mL ninhydrin solution in DMSO was added. All tubes were placed in a water bath (100 °C) for 5 min and left to cool to room temperature before adding 200 μL of 50% isopropanol to each tube. Contents in the tubes were then transferred to respective wells in 96-well plates. Absorbance was detected at 550 nm Bio Rad Model 680 Microplate Reader (Bio-Rad Laboratories, Inc., Hercules, CA, USA). Percentage of collagenase inhibition was calculated as

$$\%\ \text{collagenase inhibition} = [(\text{Abs}_{\text{control}} - \text{Abs}_{\text{sample}})/\text{Abs}_{\text{control}}] \times 100$$

where $\text{Abs}_{\text{control}}$ is the absorbance of buffer + collagenase; $\text{Abs}_{\text{sample}}$ is the absorbance of buffer + collagenase + sample/standard. All assays were carried out in triplicate and results expressed as % collagenase inhibition and/or IC_{50}, i.e., as the concentration yielding 50% of collagenase inhibition, calculated by interpolation from the % collagenase inhibition vs concentration curve.

4.3.4. Hyaluronidase inhibition assay

The methods described by Ndlovu et al.[46] and Zhou et al.[49] were applied for the hyaluronidase inhibition assay. Into 2 ml test tubes was placed: 50 μL of calcium chloride (12.5 mM), 50 μL of test samples or sodium aurothiomalate diluted in 0.1 M acetate buffer; pH 3.5 (with concentrations ranging between 9.4 and 150 μM), and 25 μL hyaluronidase (0.5 mg/ml). The tubes were incubated in a water bath (37 °C; 20 min) after which 50 μL of the substrate hyaluronic acid (0.25 mg/ml in 0.1 M acetate buffer; pH 3.5) was added and the tubes incubated for further 40 min. Twenty-five microlitres of $KBO_2 \bullet 4\ H_2O$ (0.8 M) was added to all tubes which were placed in a water bath (100 °C) for 3 min, left to cool to room temperature and 800 μL of DMAB (4 g DMAB in 40 ml acetic acid and 5 ml 10 N HCl) was added. The tubes were then incubated for 20 min and the contents transferred to respective wells in a 96-well plate. Absorbance was detected at 585 nm in a Bio Rad Model 680 Microplate Reader (Bio-Rad Laboratories, Inc., Hercules, CA, USA). Percentage of hyaluronidase inhibition was calculated as

$$\%\ \text{hyaluronidase inhibition} = [(\text{Abs}_{\text{control}} - \text{Abs}_{\text{sample}})/\text{Abs}_{\text{control}}] \times 100$$

where $\text{Abs}_{\text{control}}$ is the absorbance of buffer + hyaluronidase; $\text{Abs}_{\text{sample}}$ is the absorbance of buffer + hyaluronidase + sample/standard. All assays were carried out in triplicate and results expressed as % hyaluronidase inhibition and/or IC_{50}, i.e., as the concentration yielding 50% of hyaluronidase inhibition, calculated by interpolation from the % hyaluronidase inhibition vs concentration curve.

4.4. QSAR studies

Thirty-three xanthonic derivatives were used to construct QSAR models using the biological data obtained in *in vitro* studies (% tyrosinase inhibition, Table 2). % Inhibition was adopted as a dependent variable in the QSAR analysis. The 33 xanthones were randomly distributed into a training set (30 molecules) and a test set (3 molecules). CODESSA software (version 2.7.10, University of Florida, USA) was used to calculate more than 500 constitutional, topological, geometrical, electrostatic, quantum-chemical and thermodynamical molecular descriptors.[50] The heuristic multilinear regression procedures available in the framework of the CODESSA program were used to perform a complete search for the best multilinear correlations with a multitude of descriptors of the training set.[51] The heuristic method proceeds with a preselection of descriptors by eliminating: those descriptors that are not available for each structure; descriptors having a small variation in magnitude for all structures; descriptors found to be correlated pairwise; descriptors found to be of no statistical significance.[51,52] The two dimensional (2D)-QSAR model with the best correlation coefficient (R^2), F-test (F) and standard error (s) was selected.

4.5. Docking study

Crystal structure of *Agaricus bisporus* tyrosinase (PDB code: 2Y9X),[33] downloaded from the protein databank (PDB),[53] was used for the docking study. Structure files of the 33 test xanthones and test compound kojic acid were drawn and minimized by the semi-empirical AM1

method with Polak-Ribiere conjugate gradient (RMS < 0.1 kCal.Å^{-1}.mol^{-1}) using the chemical structure drawing tool Hyperchem 7.5 (Hypercube, FL, USA).[54] Structure-based docking was carried out using AutoDock Vina (Molecular Graphics Lab, CA, USA).[55] AutoDock Vina was run using an exhaustiveness of 8 and a grid box with the dimensions of 15.0, 20.0, and 25.0 Å, engulfing the crystallographic ligand binding site of tyrosinase.[33] Top 9 poses were collected for each molecule. The lowest docking score pose that fit the allosteric or catalytic tyrosinase binding pocket was associated with the more favourable binding conformation. PyMol1.3 (Schrödinger, NY, USA)[56] was used for visual inspection of results and graphical representations.

4.6. Statistical analysis

The assays were carried out in triplicate. The results were expressed as mean values ± standard deviations. The data was analysed using a one-way ANOVA with Tukey's test. The p-values less than 0.05 were considered statistically significant.

Funding

This research was supported by national funds through FCT, Foundation for Science and Technology, within the scope of UIDB/04423/2020 and UIDP/04423/2020 under the project PTDC/SAU-PUB/28736/2017 (reference POCI-01-0145-FEDER-028736), cofinanced by COMPETE 2020, Portugal 2020 and the European Union through the ERDF and by FCT through national funds, and supported by the Applied Molecular Biosciences Unit-UCIBIO which is financed by national funds from FCT/MCTES (UID/Multi/04378/2019). Thanks are also due to FCT, the European Union, QREN, FEDER, COMPETE, by funding cE3c center (Ref. UID/BIA/00329/2019) and Direção Regional da Ciência e Tecnologia (Azores Government) by funding Azorean Biodiversity Group.

Declaration of Competing Interest

The authors declare that they have no known competing financial interests or personal relationships that could have appeared to influence the work reported in this paper.

References

1 Rittié L, Fisher GJ. Natural and sun-induced aging of human skin. *Cold Spring Harb Perspect Med*. 2015;5.
2 Brenner M, Hearing VJ. The protective role of melanin against UV damage in human skin†. *Photochem Photobiol*. 2008;84:539–549.
3 Pillaiyar T, Manickam M, Namasivayam V. Skin whitening agents: medicinal chemistry perspective of tyrosinase inhibitors. *J Enzyme Inhib Med Chem*. 2017;32:403–425.
4 Imokawa G, Nakajima H, Ishida K. Biological mechanisms underlying the ultraviolet radiation-induced formation of skin wrinkling and sagging II: Over-expression of neprilysin plays an essential role. *Int J Mol Sci*. 2015;16:7776–7795.
5 Rinnerthaler M, Bischof J, Streubel MK, Trost A, Richter K. Oxidative Stress in Aging Human Skin. *Biomolecules*. 2015;5:545–589.
6 Farage MA, Miller KW, Elsner P, Maibach HI. Intrinsic and extrinsic factors in skin ageing: a review. *Int J Cosmet Sci*. 2008;30:87–95.
7 Papakonstantinou E, Roth M, Karakiulakis G. Hyaluronic acid: A key molecule in skin aging. *Dermato-Endocrinology*. 2012;4:253–258.
8 Ganceviciene R, Liakou AI, Theodoridis A, Makrantonaki E, Zouboulis CC. Skin anti-aging strategies. *Dermato-Endocrinology*. 2012;4:308–319.
9 Gales L, Damas AM. Xanthones-A structural perspective. *Curr Med Chem*. 2005;12:2499–2515.
10 Peres V, Nagem TJ. Trioxygenated naturally occurring xanthones. *Phytochemistry*. 1997;44:191–214.
11 Pinto MMM, Sousa ME, Nascimento MSJ. Xanthone derivatives: new insights in biological activities. *Curr Med Chem*. 2005;12:2517–2538.
12 Cidade H, Rocha V, Palmeira A, et al. In silico and in vitro antioxidant and cytotoxicity evaluation of oxygenated xanthone derivatives. *Arab J Chem*. 2017.
13 Panda SS, Chand M, Sakhuja R, Jain SC. Xanthones as Potential Antioxidants. *Curr Med Chem*. 2013;20:4481–4507.
14 Yu L, Chen L, Luo G, et al. Study on synthesis and biological evaluation of 3-aryl substituted xanthone derivatives as novel and potent tyrosinase inhibitors. *Chem Pharm Bull*. 2019;67:1232–1241.
15 Hashim NM, Rahmani M, Ee GCL, et al. Antimicrobial and tyrosinase inhibitory activities of xanthones isolated from Artocarpus obtusus F.M Jarrett. *Molecules*. 2012;17:6071–6082.
16 Chen G, Li Y, Wang W, Deng L. Bioactivity and pharmacological properties of α-mangostin from the mangosteen fruit: a review. *Expert Opin Ther Pat*. 2018;28:415–427.
17 Resende DISP, Almeida MC, Maciel B, et al. Stability, and safety evaluation of new polyphenolic xanthones towards identification of bioactive compounds to fight skin photoaging. *Molecules*. 2020;25:2782.
18 Sousa ME, Pinto MMM. Synthesis of xanthones: an overview. *Curr Med Chem*. 2005;12:2447–2479.
19 Goncalves CMA, Afonso CMM, Pinto MMM. Routes to xanthones: an update on the synthetic approaches. *Curr Org Chem*. 2012;16:2818–2867.
20 Pedro M, Cerqueira F, Sousa MEI, Nascimento MSJ, Pinto M. Xanthones as inhibitors of growth of human cancer cell lines and Their effects on the proliferation of human lymphocytes In Vitro. *Bioorg Med Chem*. 2002;10:3725–3730.
21 Lemos A, Gomes AS, Loureiro JB, et al. Synthesis, biological evaluation, and in silico studies of novel aminated xanthones as potential p53-activating agents. *Molecules*. 2019;24(10):1975.
22 Resende DISP, Pereira-Terra P, Moreira J, et al. Synthesis of a small library of nature-inspired xanthones and study of their antimicrobial activity. *Molecules*. 2020;25:2405.
23 Pinto E, Afonso C, Duarte S, et al. Antifungal activity of xanthones: evaluation of their effect on ergosterol biosynthesis by high-performance liquid chromatography. *Chem Biol Drug Des*. 2011;77:212–222.
24 Soidinsalo O, Wähälä K. Aromatic chlorination with thionyl chloride. applications in the synthesis of chlorinated isoflavones. *Phosphorus, Sulfur Silicon Relat Elem*. 2007;182(12):2761–2767.
25 Arkadiusz ZD, Tomasz A, Jorge G. Computational methods in developing quantitative structure-activity relationships (QSAR): a review. *Comb Chem High Throughput Screen*. 2006;9(3):213–228.
26 Kubinyi H. *QSAR: Hansch analysis and related approaches*. Weinheim; New York: VCH; 1993.
27 Alexander DLJ, Tropsha A, Winkler DA. Beware of R2: simple, unambiguous assessment of the prediction accuracy of QSAR and QSPR models. *J Chem Inf Model*. 2015;55(7):1316–1322.
28 Liu P, Long W. Current mathematical methods used in QSAR/QSPR studies. *Int J Mol Sci*. 2009;10:1978–1998.
29 Golbraikh A, Shen M, Xiao Z, Xiao Y-D, Lee K-H, Tropsha A. Rational selection of training and test sets for the development of validated QSAR models. *J Comput Aided Mol Des*. 2003;17:241–253.
30 Todeschini R, Consonni V. *Molecular Descriptors for Chemoinformatics*. Wiley-VCH Verlag GmbH & Co KGaA; 2009.
31 Faulon J-L, Bender A. *Handbook of Chemoinformatics Algorithms*. New York: Chapman and Hall/CRC; 2010.
32 Hall, L. H.; Kier, L. B., The Molecular Connectivity Chi Indexes and Kappa Shape Indexes in Structure-Property Modeling. 1991.
33 Ismaya WT, Rozeboom HJ, Weijn A, et al. Crystal Structure of Agaricus bisporus Mushroom Tyrosinase: Identity of the Tetramer Subunits and Interaction with Tropolone. *Biochemistry*. 2011;50:5477–5486.
34 Zhou Z, Ni D, Wang M, et al. The phenoloxidase activity and antibacterial function of a tyrosinase from scallop Chlamys farreri. *Fish Shellfish Immunol*. 2012;33:375–381.
35 Asthana S, Zucca P, Vargiu AV, Sanjust E, Ruggerone P, Rescigno A. Structure-Activity Relationship Study of Hydroxycoumarins and Mushroom Tyrosinase. *J Agric Food Chem*. 2015;63:7236–7244.
36 Jung HJ, Noh SG, Park Y, et al. In vitro and in silico insights into tyrosinase inhibitors with (E)-benzylidene-1-indanone derivatives. *Comput Struct Biotechnol J*. 2019;17:1255–1264.
37 Deri B, Kanteev M, Goldfeder M, et al. The unravelling of the complex pattern of tyrosinase inhibition. *Sci Rep*. 2016;6:34993.
38 Hassani S, Haghbeen K, Fazli M. Non-specific binding sites help to explain mixed inhibition in mushroom tyrosinase activities. *Eur J Med Chem*. 2016;122:138–148.
39 Yin SJ, Si YX, Qian GY. Inhibitory effect of phthalic Acid on tyrosinase: the mixed-type inhibition and docking simulations. *Enzyme Res*. 2011;2011, 294724.
40 Neagu E, Radu GL, Albu C, Paun G. Antioxidant activity, acetylcholinesterase and tyrosinase inhibitory potential of Pulmonaria officinalis and Centarium umbellatum extracts. *Saudi J Biol Sci*. 2018;25:578–585.
41 Wang J, Yao L. Dissecting C−H···π and N−H···π interactions in two proteins using a combined experimental and computational approach. *Sci Rep*. 2019;9:20149.
42 Resende D, Pereira-Terra P, Inácio Â, et al. Lichen Xanthones as Models for New Antifungal Agents. *Molecules*. 2018;23:2617.
43 Kimura M, Okabayashi I. Spirolactones of Xanthene. IV. New Method of Xanthone Synthesis by Oxidation of Novel Spirolactones of Dibenzo [<I>c, h</I>] xanthene and Xanthenes. *Chem Pharm Bull*. 1987;35:136–141.
44 Shimizu K, Kondo R, Sakai K, Lee S-H, Sato H. The inhibitory components from Artocarpus incisus on melanin biosynthesis. *Planta Med*. 1998;64:408–412.
45 Manosroi A, Jantrawut P, Akihisa T, Manosroi W, Manosroi J. In vitro anti-aging activities of Terminalia chebula gall extract. *Pharm Biol*. 2010;48:469–481.
46 Ndlovu G, Fouche G, Tselanyane M, Cordier W, Steenkamp V. In vitro determination of the anti-aging potential of four southern African medicinal plants. *BMC Compl Altern Med*. 2013;13:304.
47 Moore S, Stein WH. Photometric ninhydrin method for use in the chromatography of amino acids. *J Biol Chem*. 1948;176:367–388.
48 Mandl I, MacLennan JD, Howes EL, DeBellis RH, Sohler A. Isolation and characterization of proteinase and collagenase from Cl Histolyticum. *J Clin Invest*. 1953;32:1323–1329.

49 Zhou J-R, Kanda Y, Tanaka A, Manabe H, Nohara T, Yokomizo K. Anti-hyaluronidase activity in vitro and amelioration of mouse experimental dermatitis by Tomato Saponin, Esculeoside A. *J Agric Food Chem*. 2016;64:403–408.

50 Katritsky, A.; Karelson, M.; Lobanov, V.; Dennington, R.; Keith, T., CODESSA 2.7. 10. 2004.

51 Ćwik, J.; Koronacki, J. In A Heuristic Method of Model Choice for Nonlinear Regression, Rough Sets and Current Trends in Computing, Berlin, Heidelberg, 1998; Polkowski, L.; Skowron, A., Eds. Springer Berlin Heidelberg: Berlin, Heidelberg, 1998; pp 68–74.

52 Dunn WJ, Hopfinger AJ. 3D QSAR of flexible molecules using tensor representation. In: Kubinyi H, Folkers G, Martin YC, eds. *3D QSAR in Drug Design: Recent Advances*. Dordrecht: Springer, Netherlands; 1998:167–182.

53 Sussman JL, Lin D, Jiang J, et al. Protein Data Bank (PDB): Database of Three-Dimensional Structural Information of Biological Macromolecules. *Acta Crystallogr D*. 1998;54(6 Part 1):1078–1084.

54 Froimowitz M. HyperChem: a software package for computational chemistry and molecular modeling. *Biotechniques*. 1993;14:1010–1013.

55 Trott O, Olson AJ. AutoDock Vina: Improving the speed and accuracy of docking with a new scoring function, efficient optimization, and multithreading. *Int J Quantum Chem*. 2010;31:455–461.

56 Seeliger D, de Groot BL. Ligand docking and binding site analysis with PyMOL and Autodock/Vina. *J Comput Aided Mol Des*. 2010;24:417–422.